

Neutron Diffraction Study of Cathode Materials for Lithium Ion Batteries

Sumitomo Chemical Co., Ltd.
Tsukuba Research Laboratory
Toshinao SHIOYA

The neutron diffraction method is a powerful tool for analysis of inorganic crystals. This method enables us to discuss details of transition metals as well as light elements, for example lithium and oxygen, in crystals. Moreover, it is possible to analyze crystals consisting of two or more different transition metals using this method. In this paper, a brief overview of the neutron diffraction method is provided and some applications of the method to analysis of cathode materials for lithium ion batteries are shown.

This paper is translated from R&D Report, "SUMITOMO KAGAKU", vol. 2011-I

Introduction

Since lithium ion batteries have superior characteristics such as high energy density, high voltage and long cycle life, they are widely used in portable data terminal equipment starting with cellular telephones and laptop computers as well as in industrial equipment. Full-scale use of large lithium batteries is predicted for areas such as automobiles, transportation equipment, stationary energy storage, industrial machines and construction equipment in the near future.

An example of a lithium ion battery that is already in practical use is shown in Fig. 1. As shown in the figure, the configuration is one in which the cathode, the anode and the separator that isolates the two electrodes are immersed in an electrolyte; lithium ions move between the cathode and the anode, and charging and discharge

ing are carried out by oxidation-reduction reactions that occur at each of these two electrodes.

Lithium cobalt dioxide (LiCoO_2) is widely used for the cathode material. While LiCoO_2 has superior properties, there is the problem of high cost, because cobalt is a scarce element. In recent years, batteries that use manganese in the cathode materials, for which there are a wealth of reserves, nickel, which is less expensive than cobalt, and iron phosphate have been developed with the goal of reducing costs. These cathode materials take the form of composite metal oxides of lithium and transition metals, and they are used as crystals with structures suitable for lithium intercalation and de-intercalation. For example, materials with layered crystal

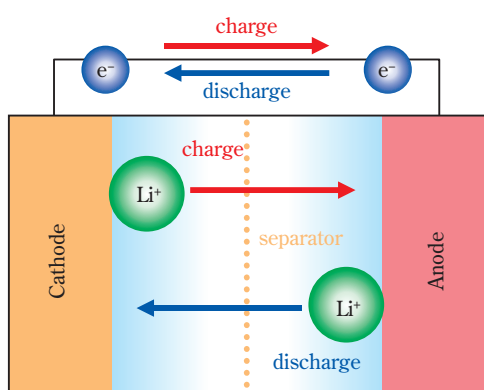


Fig. 1 Schematic of Li ion battery

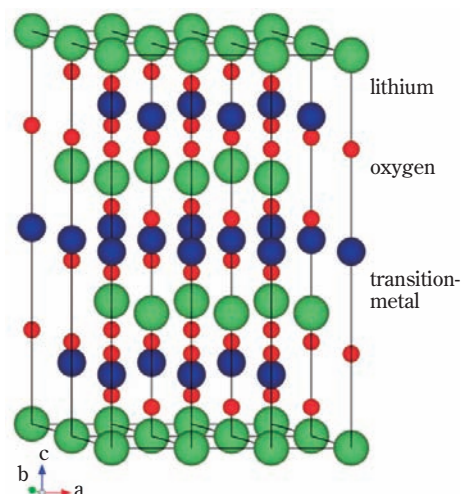


Fig. 2 Crystal structure of layered oxide

structures (Fig. 2), ones with spinel crystal structures and others have been studied.

On the other hand, graphite is widely used as an anode material, but attention is being focused on silicon materials for the next generation of materials.¹⁾ It is known that through its alloy reaction with lithium, silicon has a capacity several times to several tens of times that of graphite, but there have been problems in that the changes in volume are large and the life is short. In recent years, there have been investigations into increasing the life through the formation of complexes with carbon materials and other materials.

The separator is interposed between the cathode and the anode, and it plays the role of preventing short-circuits due to contact between the substances in the two electrodes, and also the role of assuring ion movement without releasing the electrolyte. With the increasing capacity of batteries in recent years, functions that provide heat resistance have become necessary to increase safety. As one such material, we can cite, for example, a separator (Pervio[®]) with superior heat resistance, which is a combination of a Sumitomo Chemical polyolefin based material and an aramid heat resistant layer.

To obtain a high performance lithium ion battery, the performance of each of the materials, including the cathode material, anode material, separator and electrolyte, must be improved. Fixed targets for increased performance in anode materials and electrolytes have been obtained, and we can assume that improving the performance of cathode materials will be required, particularly for increasing capacity.

Substituting different types of metal elements for some of the transition metal has been studied for improving the characteristics of cathode materials. To do so, the crystal structure of the cathode material is analyzed in detail for things such as where the substitute element enters the crystal structure and the extent of the substitution, and clarifying the relationship with battery characteristics is important for developing high-performance batteries. In addition, if we can target the analysis of the cathode material after charging and after discharging, we can expect a further acceleration of development because we will be able to relate charge and discharge phenomena to changes in crystal structure.

To analyze the crystal structure of the cathode material in detail, we must first distinguish the transition metal and also analyze lithium and oxygen, which are light elements. Methods based on neutron diffraction are suitable for distinguishing among transition metals

at the same time as light elements and as techniques that can be discussed for structural analysis. At the Tsukuba Research Laboratory, there has been a focus on neutron diffraction, and intensive effort has been put into studying analytical techniques using it. In the following we will describe the substance of these studies and give examples of applications.

Principles of Neutron Diffraction

The principles of neutron diffraction are basically the same as those for x-ray diffraction. We will leave the details of the diffraction measurements to other references,^{2),3)} and here we will give a simple explanation of the differences between the two.

Diffraction phenomena are caused by coherent scattering. The length of the coherent scattering differs with x-rays and neutrons. Since x-rays interact with the electrons and atoms, the coherent scattering length is proportional to the atomic number. Therefore, the scattering from elements that have large numbers of electrons (ones with large atomic numbers) is intense, and the scattering from light elements is weak.

Because of these properties, quantitative discussions of light elements within heavy elements and discussions that distinguish among elements with close atomic numbers are comparatively difficult.

On the other hand, since a neutron beam interacts directly with the atomic nucleus, the coherent scattering length does not depend on the atomic number. Therefore, observation of light elements within heavy elements, which is difficult with x-rays, and distinguishing transition metals with atomic numbers that are close to each other and difficult to distinguish, are comparatively easy. In addition, one of the characteristics is being able to adjust the coherent interference length by using isotopes.

Neutron diffraction has many merits, but measurements have only been carried out at limited facilities such as the Japan Atomic Energy Agency (JAEA) in Japan. However, in recent years, industrial use has become possible because of programs promoting industrial use of neutrons and shared use programs for JAEA facilities. In addition, with the startup of the Japan Proton Accelerator Research Complex (J-PARC), a time of flight (TOF) powder diffractometer (BL20, iMATERIA) has been introduced in Ibaraki Prefecture. Therefore, we have become familiar with industrial use of neutron diffraction.

A variety of information about samples is contained in a powder diffraction pattern. Crystallographic parameters such as crystal space groups and lattice constants can be obtained by carrying out Rietveld analysis using this diffraction pattern. Then, quantitative discussions of bulk crystal structures are possible. Rietveld analysis is a pattern-fitting structure-refinement method using nonlinear least-squares methods. In this method, residual errors are minimized, then, lattice and structure parameters are extracted from powder x-ray and neutron diffraction patterns (Fig. 3). See other books^{4), 5)} for details.

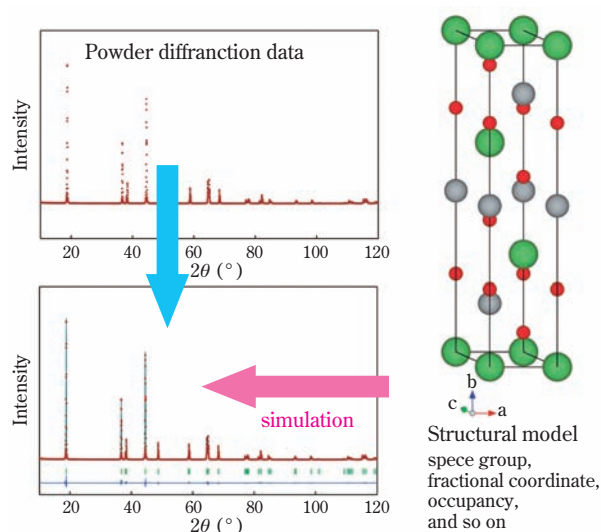


Fig. 3 Schematic of pattern fitting by Rietveld method

Here, we will describe sites and site occupancy, which have an important meaning in the analysis of crystal structures. A site is a crystallographically equivalent lattice position. When an atom is present in that lattice position, the site is said to be occupied, and that site is called an occupied site. For example, in LiCoO_2 , there are three occupied sites, and they are called the lithium site, cobalt site and oxygen site. In some cases they are called the 3a site, 3b site and 6c site. It is possible to identify crystal space groups as well as occupied sites using the previously described Rietveld analysis of powder diffraction patterns and other methods. In addition, the statistical proportion of the occupancy of an atom for that site is called the site occupancy or simply the occupancy.

Software that uses Rietveld analysis includes RIETAN-FP,⁶⁾ FullProf⁷⁾ and GSAS.⁸⁾ Among these, RIETAN-FP

is replete with Japanese information, and it is possible to visualize nuclear (electron) density using it with PRIMA, which is related software, and VESTA,⁹⁾ which was used for drawing the crystal structures for this article, and using the maximum entropy method (MEM). Software developed by the apparatus group is used in the analysis of TOF diffraction data, and it can be assumed that this role is played by Z-Rietveld, which is part of the Z-Code package¹⁰⁾ for iMATERIA.

Comparison of Neutron Diffraction and X-Ray Diffraction

As an example of an oxide containing multiple transition metal elements as described previously, we will use $\text{Li}(\text{Ni}_{1/3}\text{Co}_{1/3}\text{Mn}_{1/3})\text{O}_2$ ¹¹⁾ and describe the differences between x-ray diffraction and neutron diffraction.

The crystal structure of $\text{Li}(\text{Ni}_{1/3}\text{Co}_{1/3}\text{Mn}_{1/3})\text{O}_2$ is a layered structure as shown in Fig. 2, and nickel, manganese and cobalt are present within the transition metal layers. It is thought that the manner in which the transition metals are present within the transition metal layers has an intimate relationship with battery performance. Then, there is a need to distinguish among the transition metals in the analysis.

It has been reported that the transition metal elements (nickel, manganese and cobalt) are arranged randomly within the transition metal layers and also that they are arranged regularly.^{12), 13)} Discussion of whether or not there is regularity is generally thought to be difficult with x-ray diffraction alone. When we carried out a simulation of whether there was a difference in the x-ray diffraction pattern due to the presence or absence of regular arrangements using RIETAN-FP, almost no differences were seen. On the other hand, when neutron diffraction was used, it clearly appeared that there were differences in the diffraction pattern according to whether or not there was regularity in the way the transition metals were lined up (Fig. 4).

Example of Application

Here, we will introduce two examples of applications of neutron diffraction in analyzing the structure of lithium ion battery materials. First of all, we will introduce analysis of the charging state for $\text{Li}(\text{Ni}_{1/3}\text{Co}_{1/3}\text{Mn}_{1/3})\text{O}_2$, focusing on the lithium. Next, we will introduce an example of analyzing the structure focusing on the regularity of the transition metal arrangement.

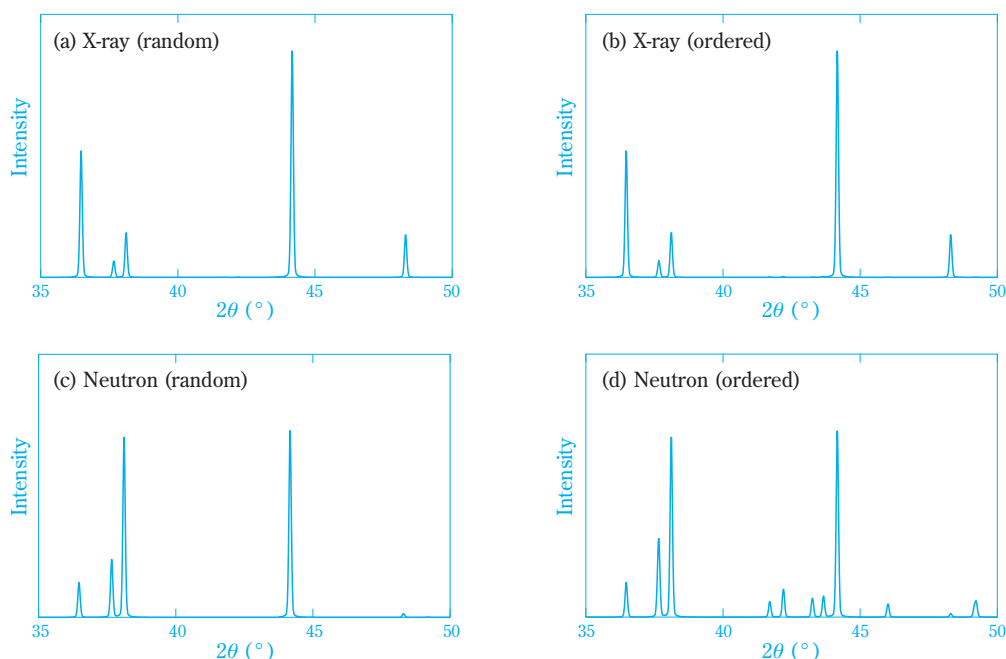


Fig. 4 X-ray diffraction simulations for $\text{Li}(\text{Ni}_{1/3}\text{Co}_{1/3}\text{Mn}_{1/3})\text{O}_2$ with (a) random or (b) ordered transition-metal layer and neutron diffraction simulations for $\text{Li}(\text{Ni}_{1/3}\text{Co}_{1/3}\text{Mn}_{1/3})\text{O}_2$ with (c) random or (d) ordered transition-metal layer

1. Crystallographic changes due to charging of $\text{Li}(\text{Ni}_{1/3}\text{Co}_{1/3}\text{Mn}_{1/3})\text{O}_2$

It is known that when the lithium is de-intercalated from the crystal by charging, crystal structures such as lattice constants change. There is an intimate relationship between the movement of lithium and the changes in the crystal structure. Therefore, we can expect to be able to clarify the charging mechanism by comparing the crystal structure in the charging state with the crystal structure before charging.

Since it is necessary to have a large amount of samples to actually analyze structural changes accompanying charging, we prepared samples that had undergone a chemical lithium extraction process¹⁴⁾ instead of charging.

Vanadium capillaries (6 mm diameter × 6 cm) were filled with the powder samples obtained, and the diffraction was measured at the J-PARC Ibaraki Materials Design Diffractometer (iMATERIA). When the neutron diffraction profiles that were obtained as a result of the measurements were compared, it was possible to confirm that the crystal structure changed with the changes in the amount of lithium from the fact that the diffraction peaks shifted with changes in the amount of lithium. The changes in the crystal structure accompanying charging can be discussed from a Rietveld analysis using these diffraction patterns.

Moreover, this analysis was carried out as a problem with publicly released results in the second half of 2010 (period 2010B) at the J-PARC Neutron Beam Line (BL) Ibaraki Materials Design Diffractometer (iMATERIA).

A phenomenon where some nickel enters the lithium layer and some lithium enters the transition metal layer has been reported because the ion radii of monovalent lithium and divalent nickel are relatively similar.¹⁵⁾ Therefore, we used a layered structural model ($[\text{Li}_{1-m}\text{Ni}_m]_{3a} [\text{Li}_m \text{Ni}_{1/3-m}\text{Co}_{1/3}\text{Mn}_{1/3}]_{3b} \text{O}_2$) for the untreated powder, and fitting was carried out by the Rietveld method using Z-Rietveld. The analysis was done with the occupancy m for nickel, which is mixed in at lattice sites (3a sites) in the lithium layer, as a variable parameter.

Fig. 5 shows the results of fitting with the diffraction patterns. The neutron diffraction patterns from measurements (red + in the upper part) and calculations (solid blue line in the upper part) are shown with the difference for the two below. Moreover, the broad peaks from 18200 sec to 19400 sec and 31390 sec and the comparatively sharp peaks at 21455 sec and 30340 sec are caused by the background of the apparatus itself and the vanadium holders; therefore there were no peaks originating in the samples. Excellent fitting was obtained, and it can be assumed that the untreated $\text{Li}(\text{Ni}_{1/3}\text{Co}_{1/3}\text{Mn}_{1/3})\text{O}_2$ has a type R-3m space group

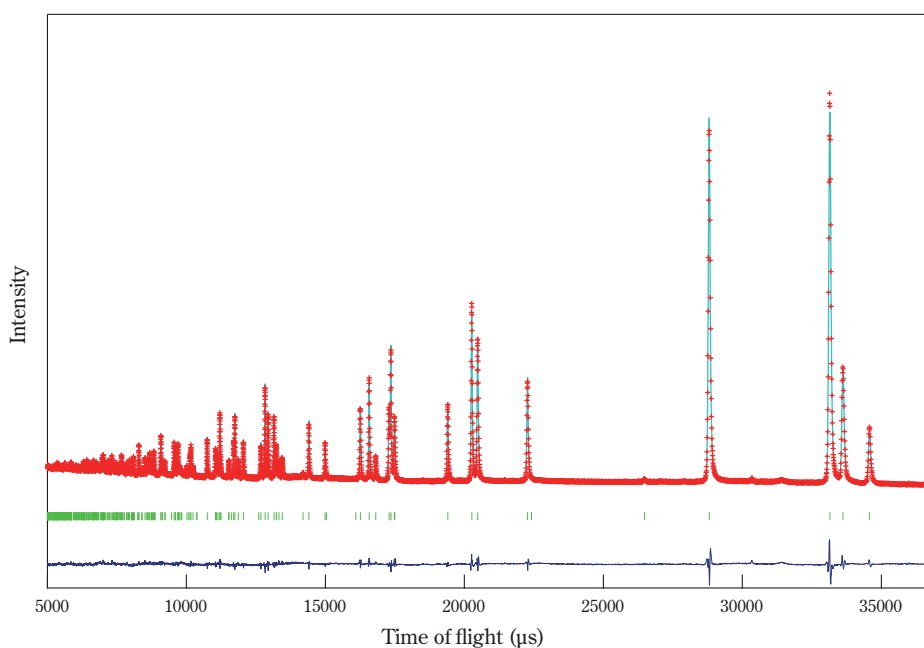


Fig. 5 Rietveld fitting patterns of the neutron diffraction data for the pristine $\text{Li}(\text{Ni}_{1/3}\text{Co}_{1/3}\text{Mn}_{1/3})\text{O}_2$. Plus marks (red) are the observed data and the solid line (blue) is the calculated profile. The bottom line shows the difference between the observed and the calculated patterns.

crystal structure with layering of a lithium-oxygen octahedral layer and a transition metal (nickel, manganese and cobalt)-oxygen octahedral layer.

Next, we carried out pattern fitting using the Rietveld method on treated powder to analyze the crystal structure after the lithium extraction process. Here, we used a structural model given by $[\text{Li}_{n1}\text{Ni}_m]_{3a} [\text{Li}_{n2}\text{Ni}_{1/3-m}\text{Co}_{1/3}\text{Mn}_{1/3}]_{3b}\text{O}_2$ and set the crystal structure of the untreated powder as the initial structure. Here, the occupancies for the transition metal elements (nickel, manganese and cobalt) were fixed at the analytical results for the untreated powder, and only the lithium (3a) site and

transition metal (3b) site lithium occupancy ($n1$, $n2$) were allowed to increase in precision. **Fig. 6** shows the lithium occupancy for the 3a site and 3b site as a function of the amount of lithium extracted (x). It can be seen that most of the lithium has gone out of the lithium layer, and some of the lithium in the transition metal layer has escaped. With x-ray diffraction it is difficult to examine precisely what site the lithium has escaped from, but by using neutron diffraction is possible to quantitatively discuss the escape from the transition metal layer.

On the other hand, it can be seen that the $\text{Li}(\text{Ni}_{1/3}\text{Co}_{1/3}\text{Mn}_{1/3})\text{O}_2$ expanded along the c-axis with a reduction of the lithium in the crystal by charging. When the changes in crystal structure accompanying charging and discharging are large, there is a danger of the electrode structure deteriorating with a breakdown in the junction with the conductor and other problems; therefore, we can assume that it is preferable to have smaller changes (elongation along the c-axis) in the crystal structure of the active material in the cathode. If we look at the crystal structure before and after charging from this point of view, the transition metal layer thickness is reduced, while the thickness of the lithium layer increases approximately 1.5 fold as the amount of lithium extracted (x) increases by charging, as is shown in **Fig. 7**. Here, the distance between the oxygen layers and-

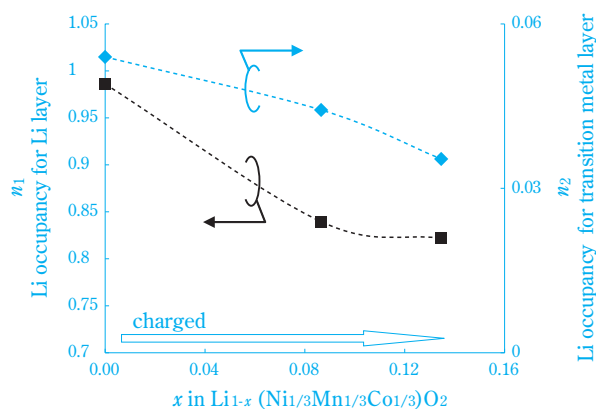


Fig. 6 Li occupancy of (■) the Li site and (◆) the transition metal site as a function of an amount of extracted lithium

wiching the lithium layer and transition metal layer vertically is called the thickness of the lithium layer and the transition metal layer. Therefore, it can be assumed that to reduce the structural changes due to charging, it will be effective to control the thickness of the lithium layer, which changes with charging. Thus, if neutron diffraction which can examine the positions of the oxygen atoms in a crystal that includes transition metals in detail on the atomic level is used, there is a great deal of crystallographic information not only from the lithium, but also from the oxygen.

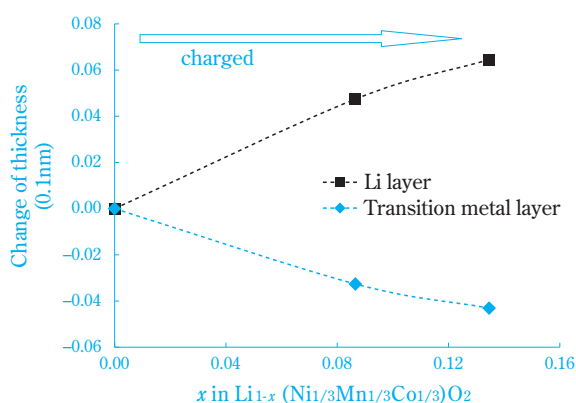


Fig. 7 Thickness of (■) the lithium layer and (◆) the transition metal layer as a function of an amount of extracted lithium

2. Crystallographic changes accompanying charging and discharging of hydrothermal cathode materials

Compared with the dry methods that are typically widely used as methods for synthesizing inorganic compounds, the synthesis temperature with a hydrothermal method is low at roughly 150°C to 200°C. In addition, since the reaction occurs in a water solvent, it is possible to synthesize inorganic powders with little aggregation of the fine particles. In the cathode materials used for lithium ion batteries, mobile ions of lithium move in and out of the crystal from the surface of the cathode material particles which are in contact with the electrolyte. Therefore, it can be assumed that it would be advantageous to design cathode materials with large specific surface areas as a method for obtaining high capacity cathode materials. After investigating the various conditions, the possibility of synthesizing a fine particle, layered nickel-manganese cathode material by hydrothermal methods was confirmed.¹⁶⁾ Furthermore, the singular behavior of the charge and discharge capacity increasing (up to 200 mAh/g) with charge and dis-

charge cycles at 60°C for the hydrothermal cathode material was found. This behavior is peculiar to hydrothermal cathode materials, and it is expected that it will play an important role in the guidelines for development of high-capacity cathode materials with the clarification of the mechanism for increasing the capacity. Therefore, we carried out a crystal structural analysis before and after charging to get at the causes of this increase in capacity.

(1) Structure of hydrothermal cathode material before charging

The cathode material composition obtained by the hydrothermal method had a Li:Ni:Mn:Co mole ratio of 1.40:0.40:0.49:0.10 from chemical composition analysis using induction coupled plasma (ICP) emission spectrochemical analysis. Neutron diffraction measurements were carried out on this powder using the Japan Atomic Energy Agency (Tokai-mura) High Resolution Powder Diffractometer (HRPD).

In x-ray diffraction, diffraction peaks were observed in the neighborhood of $2\theta = 21^\circ - 23^\circ$ (Cu-K α radiation source) for the hydrothermal cathode material. These peaks are not seen when the transition metals are disordered in the transition metal layer. Thus, these peaks indicate the presence of a superlattice structure of the transition metal layer. Moreover, it is assumed that the space group belongs to C2/m (monoclinic). Therefore, we carried out a Rietveld analysis based on the diffraction data obtained in measurements using a structural model for a C2/m space group (monoclinic crystal) with an ordered transition metal layer. The refined crystallographic parameters are shown in **Table 1**. Here, this Rietveld analysis made use of RIETAN-FP. As a result, the cathode material obtained by the hydrothermal method can be given by $[\text{Li}]_{4h}[\text{Li}_{0.5}]_{2c}[\text{Li}_{0.225}\text{Ni}_{0.147}\text{Co}_{0.128}]_{2b}[\text{Ni}_{0.362}\text{Mn}_{0.638}]_{4g}[\text{O}_{1.0}]_{4i}[\text{O}_{2.0}]_{8j}$. **Fig. 8 (a)** shows a schematic diagram of the arrangement of atoms within the transition metal layer in the uncharged state. We found that nickel and manganese are present in the honeycomb skeleton (4g sites) at proportions of 36% and 64%, respectively. In addition, lithium, nickel and cobalt were clearly present in proportions of 45%, 29% and 26% at the center of the honeycomb (2b sites). In other words, we found that there was a characteristic structure within the transition metal layer where cobalt is only present at the center of the honeycomb, and on the other hand, manganese is only present in the honeycomb skeleton.

Table 1 Crystallographic parameters for (a) the pristine and (b) the discharged cathode active materials via the hydrothermal reaction obtained by the Rietveld analysis. The fractional coordinates, x, y, z are shown in the fourth, fifth, sixth column, respectively. Isotropic displacement parameters, B, are shown in the last column.

before charge

| Atom | Site | occupancy | number of atoms per unit formula | x | y | z | B [0.01nm ²] |
|------|------|-----------|----------------------------------|-----------|-----------|-----------|--------------------------|
| Li | | 0.450(2) | 0.225 | | | | |
| Ni | 2b | 0.294(2) | 0.147 | 0 | 1/2 | 0 | 4.0(3) |
| Co | | 0.256(2) | 0.128 | | | | |
| Mn | | 0.000(2) | 0.000 | | | | |
| Li | | 2c | 1 | | | | |
| Li | 4h | 1 | 1 | 0 | 0.656(1) | 1/2 | 1.4(2) |
| Li | | 0.000(2) | 0.000 | | | | |
| Ni | 4g | 0.362(2) | 0.362 | 0 | 0.162(1) | 0 | 0.19(2) |
| Co | | 0.000(2) | 0.000 | | | | |
| Mn | | 0.638(2) | 0.638 | | | | |
| O | | 4i | 1 | | | | |
| O | 8j | 1 | 2 | 0.2503(5) | 0.3256(2) | 0.2236(4) | 0.55(4) |

after discharge

| Atom | Site | occupancy | number of atoms per unit formula | x | y | z | B [0.01nm ²] |
|------|------|-----------|----------------------------------|----------|-----------|----------|--------------------------|
| Li | | – | – | | | | |
| Ni | 2b | 0.422(5) | 0.211 | 0 | 1/2 | 0 | 0.13(5) |
| Co | | 0.24(5) | 0.120 | | | | |
| Mn | | 0.080 | 0.040 | | | | |
| Li | | 2c | 0.08 | | | | |
| Li | 4h | 1.00 | 1.00 | 0 | 0.668(9) | 1/2 | 0.13(5) |
| Li | | – | – | | | | |
| Ni | 4g | 0.289(5) | 0.289 | 0 | 0.1686(9) | 0 | 0.13(5) |
| Co | | 0.018(5) | 0.018 | | | | |
| Mn | | 0.573 | 0.573 | | | | |
| O | | 4i | 1 | | | | |
| O | 8j | 1 | 2 | 0.231(2) | 0.328(2) | 0.245(1) | 0.16(3) |

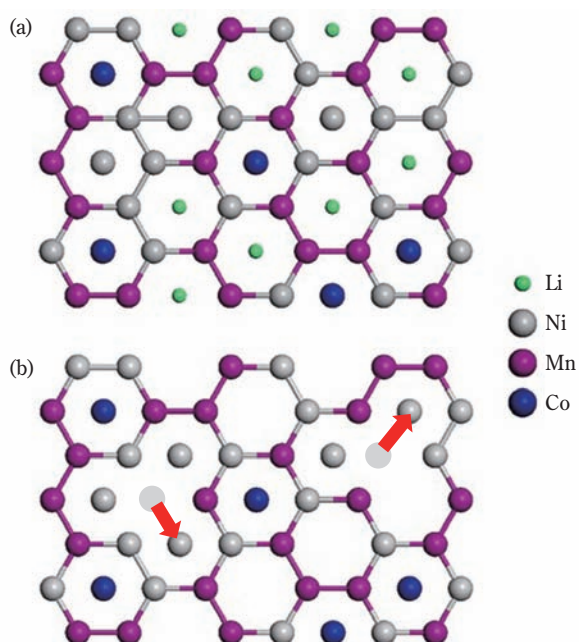


Fig. 8 Schematic of transition metal layers for (a) the pristine and (b) the discharged cathode active materials via the hydrothermal reaction.

(2) Structure after charging and discharging of hydrothermal cathode material

The cathode material composition obtained by the hydrothermal method was charged at 60°C until the voltage reached 4.5V and was then held at 4.5V, which is so-called constant current and constant voltage (CCCV) charging. The cell was discharged to 3.0V at constant current. After discharging, the cell was charged at CCCV to 4.5V and discharged to 3.0V again. Subsequently, the cell was charged at CCCV to 4.3V and discharged to 3.0V. Finally, discharged powder was recovered. Moreover, the mole ratios of Li:Ni:Mn:Co composition from ICP emission spectrochemical analysis were 0.83:0.40:0.49:0.11.

The discharged powder was a mixture of cathode material, conductor material and binder. In neutron diffraction, diffraction from carbon, which is contained in the conductor material and binder, cannot be ignored. On the other hand, in x-ray diffraction analysis, diffraction is affected little by carbon. Therefore, to improve

the precision of the analysis, the x-ray diffraction analysis and the neutron diffraction analysis were carried out alternately. Using this method, we refined the crystallographic parameters.¹⁷⁾

First, we carried out an x-ray diffraction Rietveld analysis for a structural model where all of the lithium in the transition metal layer had escaped from the structure of the uncharged state (C2/m space group). Here, we considered the case where the transition metal moves during charging and discharging, and we calculated the fractional coordinates for each site and the unoccupied rate for 4g sites. Here, the unoccupied rate is the proportion of the lattice points where no atoms are present. After that, we alternately refined each structural parameter using neutron diffraction and x-ray diffraction Rietveld analysis. As a result, we obtained the crystallographic parameters given in **Table 1**. **Fig. 8** (b) shows a schematic diagram of the arrangement of atoms within the transition metal layer after charging and discharging. It is clear that nickel, manganese and cobalt are present in the honeycomb skeleton (4g sites) at proportions of 29%, 57% and 2%, respectively, and nickel, manganese and cobalt are present in proportions of 42%, 8% and 24% at the honeycomb centers (2b sites). In addition, it was found that 26% and 12%, respectively, of the honeycomb centers and honeycomb skeleton were unoccupied.

Comparing the crystal structures before charging and after charging and discharging, it was found that some atoms moved within the transition metal layer in association with increase in discharge capacity. Most of that movement was found to be by nickel (**Fig. 8**). We think that it is necessary to move forward with investigations into the relationship between these structural changes and the increased capacity in the future.

Conclusion

In this article, we introduced the use of powder neutron diffraction in structural analysis of cathode materials for lithium ion batteries. To analyze in detail the cathode materials, which are crystals of transition metal oxides that include lithium, we must analyze lithium and oxygen, which are light elements as well as distinguishing among transition metals in the first place. Neutron diffraction, which makes possible discussion of light elements within heavy elements and makes it comparatively easy to distinguish among transition metals, is a powerful tool. Moving forward, we feel that neutron

diffraction technology will play an important role in forwarding the development of high-performance cathode materials.

Finally, we would like to discuss the future outlook for industrial use of neutrons. In conventional angular variance diffraction measurements, the amount of sample necessary for measurements was several grams, but the high-intensity TOF diffractometer (iMATERIA) can be thought of as oriented towards industrial use. In addition, it is running at approximately 200 kW at present, but typically, measurements can be performed in roughly 15 to 30 minutes per sample. For example, for samples where the firing temperature and composition are varied exhaustively, it is possible to measure all of them in a short period of time. It is easily possible to use it in the same manner as x-ray diffraction measurements in a normal laboratory, and it has become a powerful means of analysis for industrial use. When it moves to megawatt operations in the future, we can expect the throughput to improve even more. In addition, there are predictions of developing in-situ tests during the charging of batteries, which would have been difficult with angular variance by using a high intensity neutron source, and there are expectations for elucidating charging and discharging mechanisms.

Moreover, the J-PARC neutron beam line suffered great damage because of the Great East Japan Earthquake on March 11, 2011. The damage to various equipment and apparatus was large, and it is estimated that it will be a long time before they began operating again. Currently, exhaustive efforts are being made at restoration work, and we are hoping for restoration as soon as possible.

References

- 1) R. Ruffo, S. S. Hong, C. K. Chan, R. A. Huggins and Y. Cui, *J. Phys. Chem. C*, **113**, 11390 (2009).
- 2) Sakurai Toshio, X-sen Kessho Kaiseki no Tebiki [A Practical Guide for X-ray Crystal Structure Analysis], Shokabo (1983).
- 3) Waseda Yoshio and Matsubara Eichiro, X-sen Kouzo Kaiseki Genshi no Hairetsu wo Kimeru [X-ray Structure Analysis Determination of Atomic arrangement], Uchida Rokakuho (1998).
- 4) Izumi Fujio, Zikken Kagaku Kouza 11 Busshitsu no Kouzo III Kaisetsu Dai 5 han [The Fifth Series of Experimental Chemistry 11 Structure of Matter III Diffraction], Maruzen (2006).

- 5) Nakai Izumi and Izumi Fujio, *Funmatsu X sen Kaiseiki no Zissai dai 2 han* [Actuals of X-ray analysis, the second edition], Asakura Shoten (2009).
- 6) F. Izumi and K. Momma, *Solid State Phenom.*, **130**, 15 (2007).
- 7) J. Rodriguez-Carvajal, *Newsletter*, **26**, 12 (2001).
- 8) A.C. Larson and R.B. Von Dreele, *Los Alamos National Laboratory Report LAUR*, **2000**, 86-748.
- 9) K. Momma and F. Izumi, *J. Appl. Crystallogr.*, **41**, 653 (2008).
- 10) R. Oishi, M. Yonemura, Y. Nishimaki, S. Torii, A.Hoshikawa, T. Ishigaki, T. Morishima, K. Mori and T. Kamiyama, *Nucl. Instrum. Meth. Phys. Res. A*, **600**, 94-96 (2008).
- 11) T. Ohzuku and Y. Makimura, *Chemistry Letters*, **2001**, 642.
- 12) Y. Koyama, I. Tanaka, H. Adachi, Y. Makimura and T. Ohzuku, *J. Power Sources*, **119-121**, 644 (2003).
- 13) N. Yabuuchi, Y. Koyama, N. Nakayama and T. Ohzuku, *J. Electrochem. Sos.*, **152**, A1434 (2005).
- 14) W. Tang, H. Kanoh and K. Ooi, *J. Solid State Chem.*, **142**, 19 (1999).
- 15) E. Rossen, C.D.W. Jones and J.R. Dahn, *Solid State Ionics*, **57**, 311 (1992).
- 16) Imanari Yuichiro, Isobe Toshinori, Nakane Kenji, Tabuchi Mitsuharu and Tatsumi Kuniaki, The 51st Battery Symposium in Japan, 2C03 (2010).
- 17) Sumitomo Chemical Co., Ltd., Jpn. Kokai Tokyo Koho 2010-14414(2010).

PROFILE



Toshinao SHIOYA

Sumitomo Chemical Co., Ltd.
Tsukuba Research Laboratory
Research Associate, Ph. D